

The Influence of Cooling Rate on the Microstructure and Microsegregation in Al–30Sn Binary Alloy

A. R. Valizadeh · A. R. Kiani-Rashid ·
M. H. Avazkonandeh-Gharavol · E. Z. Karimi

Received: 21 December 2012/Revised: 11 February 2013/Accepted: 16 February 2013/Published online: 6 March 2013
© Springer Science+Business Media New York and ASM International 2013

Abstract Aluminum–tin alloys have wide industrial uses, especially in tribological applications. Their structure is consisted of Al- α dendrites (bearing the mechanical load) surrounded by Sn-rich interdendritic layers that function as a solid lubricant. Despite extensive research on solidification behavior of Al–Sn and Al–Sn-based alloys, microsegregation is not yet fully understood. The aim of this article is to study the effect of cooling rate on the microsegregation of Al–30 wt% Sn. Three cooling rates including 3.5, 12.3, and 95.8 K/s were achieved by using three various molds made of sand, brass, and water-cooled brass with the same respective die hole geometries. The results showed that the microstructure becomes much finer with increasing cooling rate. The minimum concentration of Sn in Al was increased by increasing cooling rate approximately four times of equilibrium concentration. The hardness increased mainly as a result of microstructure refinement.

Keywords Aluminum · Tin · Cooling rate · Microstructure · Microsegregation

Introduction

Aluminum–tin alloys are well known for having excellent tribological and mechanical properties making them suitable for engineering applications, particularly in combustion engine pistons and cylinder liners [1]. As can be seen in Fig. 1 [2], the solid solubility limit of Sn in Al is below 0.09 wt% Sn (0.02 at% Sn); therefore, Al–Sn alloys, which have Sn contents higher than 0.09 wt%, are formed by Sn particles spread over a continuous Al-rich matrix. This type of structural morphology determines the good tribological behavior of the alloy because of the tough Al-rich matrix, which is more resistant to high mechanical loads. The structure acts in combination with the Sn particles that function as solid lubricants [3]. Conventional Babbitt alloys, especially lead bronzes alloys, are increasingly being replaced by aluminum alloys, particularly in the automobile industry [4]. Such alloys are also recommended as anodic protective coatings for anti-corrosive protection of steel [5].

Cruz et al. [1, 3, 6] worked on the solidification structure of Al–Sn alloys directionally solidified under transient heat flow conditions. Combined theoretical and experimental approaches have been used to quantitatively determine thermal variables such as (a) transient metal/mold heat transfer coefficients, (b) tip growth rates, (c) thermal gradients, (d) tip cooling rates, and (e) local solidification time. This study focuses on the dependence of dendrite arm spacing on the alloy solute content and thermal variables [1]. The effects of cooling rate on solidification structure and hence tensile and wear properties were also investigated [3]. Cruz et al. [6] also studied the inverse (macro-) segregation of Al–23% Sn directionally solidified under transient heat flow conditions experimentally and by finite volume numerical modeling [6]. Kliauga and Ferrante [7] added 0.5 wt% Sn to A356 commercial Al alloy and

A. R. Valizadeh (✉)

Department of Materials Engineering, Science and Research Branch, Islamic Azad University, Tehran, Iran
e-mail: engr.alireza.valizadeh@gmail.com

A. R. Kiani-Rashid · M. H. Avazkonandeh-Gharavol
Department of Materials Engineering and Metallurgy, Faculty of Engineering, Ferdowsi University of Mashhad, Mashhad, Iran

E. Z. Karimi
Department of Metallurgy, Islamic Azad University, Mashhad Branch, Mashhad, Iran

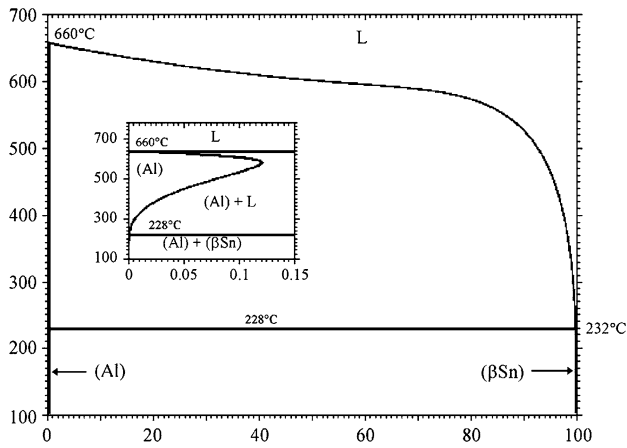


Fig. 1 Al–Sn phase diagram [2]

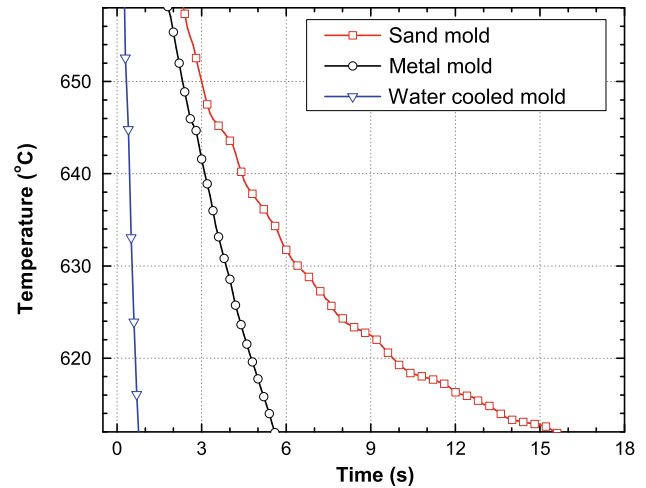
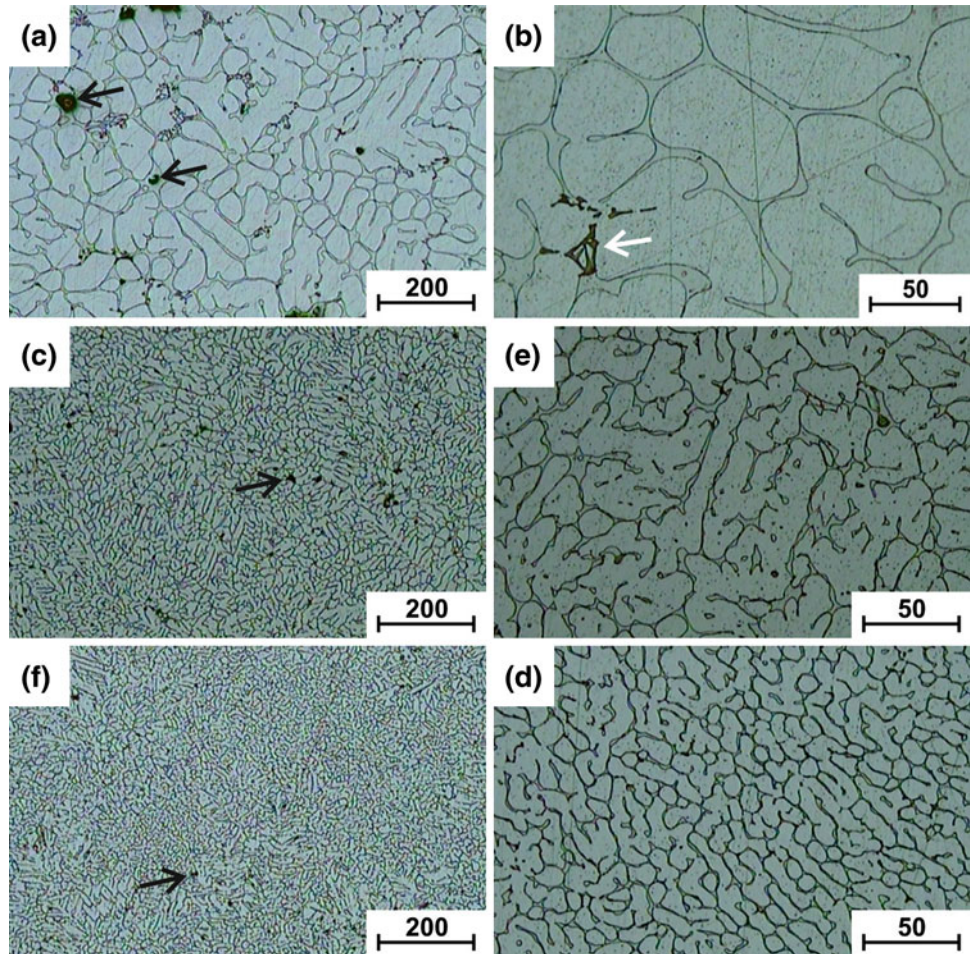


Fig. 2 Measured cooling curves for the different cooling conditions in the range 660–610 °C

Fig. 3 Optical micrographs showing microstructures of samples casted in (a, b) sand; (c, d) metal; and (e, f) water-cooled metal molds with different magnifications. The third phase and the holes are indicated by white and black arrows, respectively



observed that Sn reduced the contiguity and the growth kinetics of the Al- α particles and contributed to grain orientation randomizing.

Extensive research has been conducted on different aspects of solidification processing of Al–Sn and Al–Sn-based alloys

including dendrite arm spacing [1, 3, 8], simulation of structure formation during solidification [6, 9], columnar-to-equiaxed transition in directional solidification [10, 11], and on the effects of other alloying elements on the solidification behavior of binary Al–Sn alloys [12–16]. Despite the wide

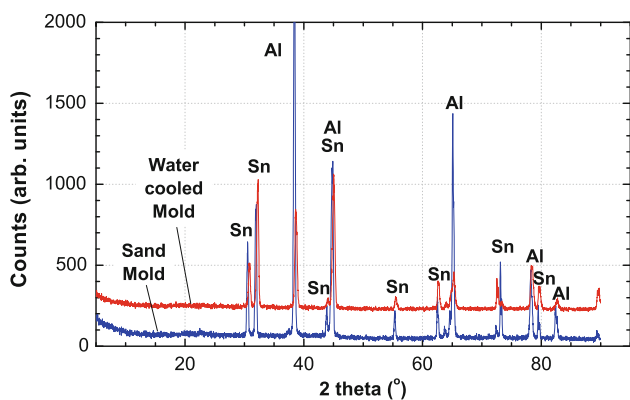


Fig. 4 XRD spectra from the samples produced with the two extreme cooling conditions

use of Al–Sn alloys for engineering applications, studies conducted on the microsegregation of such materials are few. Increasing cooling rate was reported to increase solid solubility and hence decrease the microsegregation and therefore the second phase content [17, 18]. More alloying elements will remain in the primary Al- α dendrites that strengthen them by solid solution hardening. Increasing cooling rate also decreases the scale of microstructure, which in turn increases the strength of the alloy. Both these effects are beneficial because the application of the current alloy in tribological applications needs to be stronger. Cooling rate range in industrial casting processes can be as low as 0.01 K/s for massive sand casting, and also can be as high as 10^5 K/s upon rapid solidification of granules and flakes. The majority of casting processes, however, operate in the range of cooling rates between 0.1 and 20 K/s [19]. The aim of the current research is to study the effect of cooling rate on the microstructure and specially microsegregation of the Al–Sn binary alloy in a common cooling rate range in industry.

Experimental Procedure

An Al alloy containing approximately 30 wt% Sn was produced by melting high purity Al (99.99%) and Sn (purity higher than 99.5%) by a resistance furnace in air in an alumina crucible. The chemical composition of the alloys was determined using atomic absorption technique. The alloy was cast using three different mold materials to produce three different cooling rates. A silica sand mold was used for low cooling rate and a metallic (brass) mold with and without water circulation was used as two other cooling conditions with higher cooling rates. All molds had a cylindrical hole with the same size of $D \times H$: 2 × 2 cm. During casting, the cooling curves were saved by a data acquisition system using a 0.5 mm diameter K thermocouple. After being cooled to

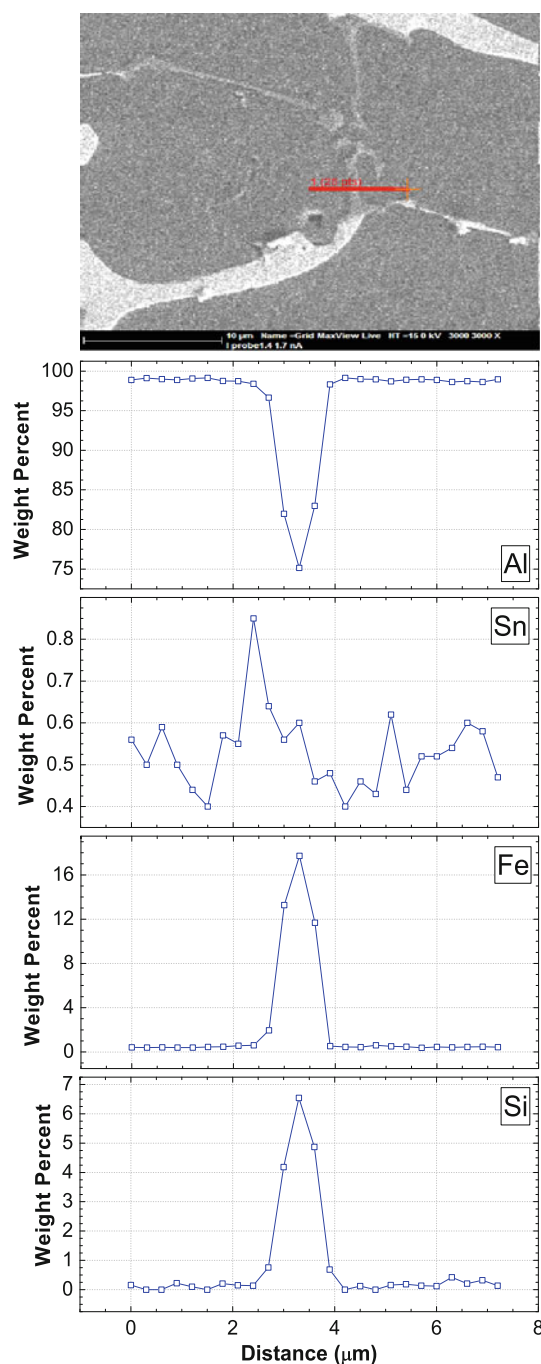


Fig. 5 Elemental concentration profiles for third type phases in sample casted in sand mold

room temperature, samples were cross sectioned and prepared for metallography, microhardness, electron probe micro-analysis (EPMA), and x-ray diffraction (XRD) examination. Metallography of samples was performed according to conventional procedures, with grinding and then polishing with micron sized diamond paste on a rotating wheel. The samples were etched in Keller’s reagent to reveal their microstructures. The microstructures of etched samples

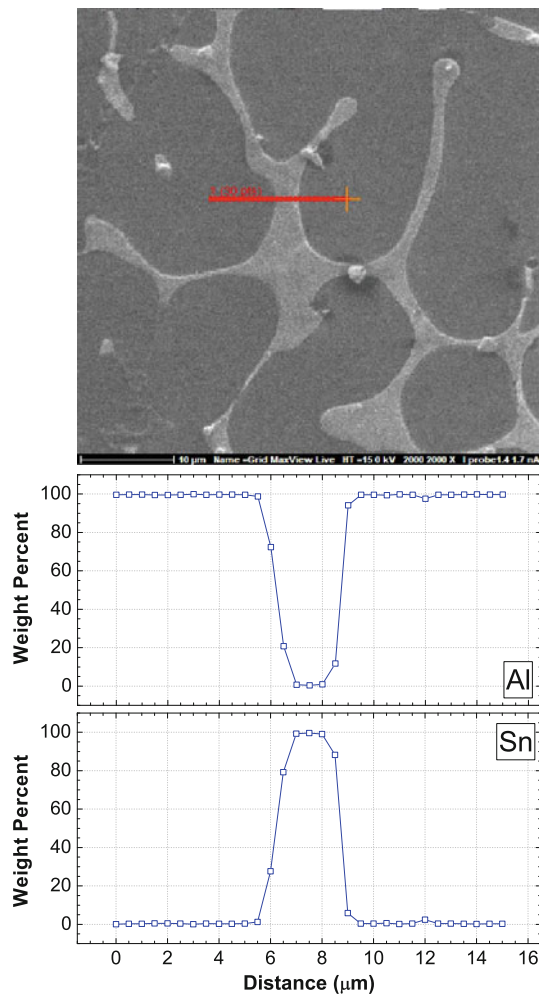


Fig. 6 SEM micrograph and line scan analysis for the sample casted in sand mold

were studied via light microscopy. The quantity of the second phase was measured by processing light micrographs. The hardness of the samples was determined using a microhardness tester with a 200 g load. XRD was used to identify the phases present in the as-cast microstructure. The grain size of the samples was also measured from XRD spectra. Microsegregation was studied with EMPA line scans on etched samples.

Results and Discussion

The chemical composition as determined by atomic absorption analysis was 69.93 wt% Al and 30.02 wt% Sn; the impurity level was approximately 0.05 wt%. The cooling rate is calculated in the range of 660–610 °C according to the curves shown in Fig. 2. This figure shows that changing the mold material from sand to water-cooled brass significantly changed the cooling rate of the melt.

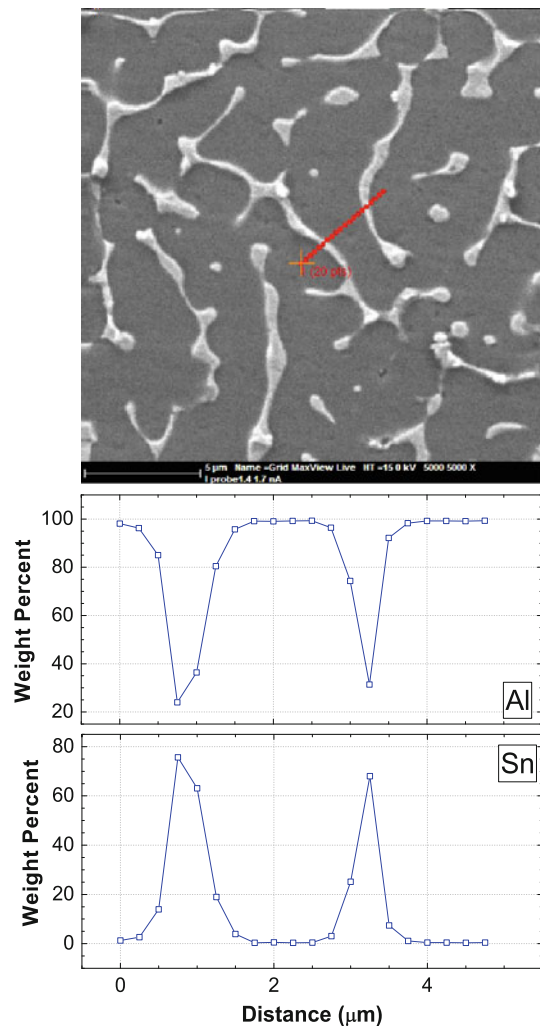


Fig. 7 SEM micrograph and line scan analysis for the sample casted in metal mold

The cooling rates calculated from the cooling curves were 3.5, 12.3, and 95.8 K/s for the samples casted in sand, metal, and water-cooled metal mold, respectively.

The microstructures of all samples are shown in Fig. 3. The microstructure consists of two phases: a dendritic Al-rich phase and a Sn-rich interdendritic phase. These phases were also confirmed by XRD analysis that consisted of two peak sets as indicated in Fig. 4. The microstructure became finer with increasing cooling rate, as shown in Fig. 3. Increasing the cooling rate increased the undercooling of the melt and the solidification began at a lower temperature. At lower temperatures, however, the diffusion was limited and the rate of nucleation was increased because of higher driving forces. The structures therefore became finer as the cooling rate increased.

Many large pores, which were mostly localized to the Sn-rich phase, were observed in the sand mold casting sample. Increasing the cooling rate reduced both the number and the size of these pores. This sample also

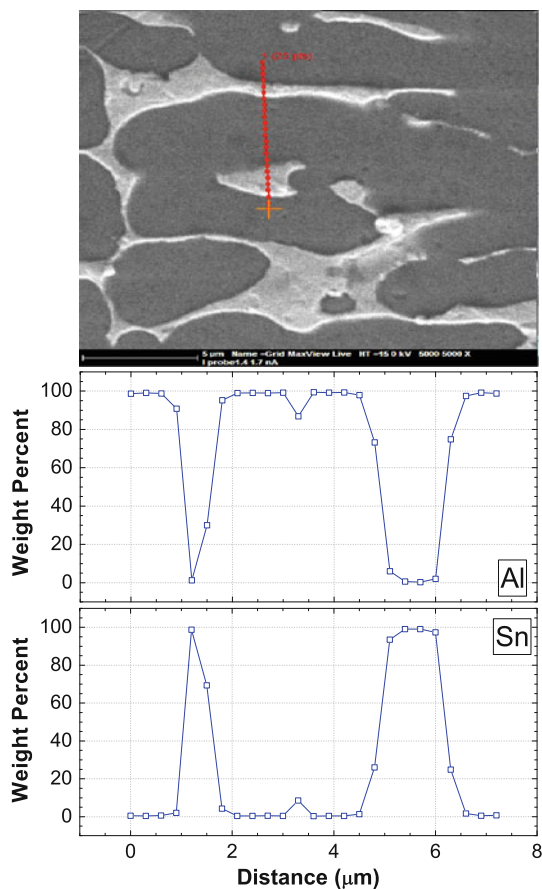


Fig. 8 SEM micrograph and line scan analysis for the sample casted in water-cooled metal mold

Table 1 Structural features of samples

Mold	Coolingrate (K/s)	Second phase content	C_{min} (wt%)	Vickers hardness
Sand mold	3.5	16.6	0.08	29.1
Brass mold	12.3	18.5	0.34	31.1
Water-cooled brass mold	95.8	15.5	0.29	33.8

contains a third phase in addition to the Al- and Sn-rich phases. This phase has a plate-like morphology with Chinese script shape. The EPMA results shown in Fig. 5 revealed that this phase contains iron and silicon, in addition to aluminum and tin. The Sn concentration profile shows no preferential segregation to this phase. All samples were cast from the same master alloy, but this phase was only observed in the sand mold sample. It is possible that silica from the mold became incorporated in the alloy. The concentration of this phase was low (approximately 4%) and thus it was not detected via XRD.

The results of EPMA line scan analyses are presented in Figs. 6–8. This analysis was used to compare the level of

microsegregation for the different cooling rates. Minimum solute concentration was used as the criterion of microsegregation; with increasing minimum concentration of Sn in Al dendrites, the level of microsegregation was decreased. The minimum concentration for each cooling rate is reported in Table 1. In the lowest cooling rate, the Sn content of the Al dendrites was 0.08 wt% which was similar to the theoretical value of 0.09 wt%. By increasing the cooling rate, the minimum Sn concentration was increased approximately four times up to 0.34 wt%. The microsegregation first decreased and then increased again in the water-cooled brass mold.

The results of the hardness test are also shown in Table 1. Hardness increased monotonically with increasing cooling rate. The only parameter that was correlated with hardness was microstructure refinement (Fig. 3; Table 1). The grain size calculated from XRD analysis was 535 µm for the sand mold sample and 146 µm for the water-cooled brass sample, and shows a reduction of grain size by increasing the cooling rate. The conventional Babbitt alloys are being replaced by Al–Sn alloys because of their superior mechanical properties; Al–Sn alloys can withstand substantially higher loads than the Babbitt alloys [4]. The ability to increase hardness by increasing the cooling rate has useful implications for the continued adoption of these alloys.

Conclusions

The effect of cooling rate on the microstructure and microsegregation in Al–30 wt% Sn was studied by means of quantitative metallography and EPMA. The main conclusions drawn from this study were that with increasing cooling rate, the microstructure became finer and the minimum solute concentration increased to approximately four times the equilibrium value. Hardness also increased with cooling rate, mainly as a result of microstructure refinement.

References

1. K.S. Cruz, J.E. Spinelli, I.L. Ferreira, N. Cheung, A. Garcia, Microstructural development in Al–Sn alloys directionally solidified under transient heat flow conditions. *Mater. Chem. Phys.* **109**(1), 87–98 (2008)
2. ASM Handbook Committee, Alloy phase diagrams, in *ASM Handbook*. vol 3 (ASM International, Ohio, 1992)
3. K.S. Cruz, E.S. Meza, F.A.P. Fernandes, J.M.V. Quaresma, L.C. Casteletti, A. Garcia, Dendritic arm spacing affecting mechanical properties and wear behavior of Al–Sn and Al–Si alloys directionally solidified under unsteady-state conditions. *Metall. Mater. Trans. A* **41**(4), 972–984 (2010)
4. T. Stuczynski, Metallurgical problems associated with the production of aluminum–tin alloys. *Mater. Des.* **18**(4–6), 369–372 (1997)

5. W.R. Osorio, J.E. Spinelli, N. Cheung, A. Garcia, Secondary dendrite arm spacing and solute redistribution effects on the corrosion resistance of Al–10 wt% Sn and Al–20 wt% Zn alloys. *Mater. Sci. Eng. A* **420**(1–2), 179–186 (2006)
6. K.S. Cruz, I.L. Ferreira, J.E. Spinelli, N. Cheung, A. Garcia, Inverse segregation during transient directional solidification of an Al–Sn alloy: numerical and experimental analysis. *Mater. Chem. Phys.* **115**(1), 116–121 (2009)
7. A.M. Kliauga, M. Ferrante, The influence of Sn on texture and grain growth of an Al7Si0.3Mg alloy (A356) in the semi-solid state. *Jornadas SAM-CONAMET-AAS*, pp. 83–90 (2001)
8. T. Okamoto, K. Kishitake, Dendritic structure in unidirectionally solidified aluminum, tin, and zinc base binary alloys. *J. Cryst. Growth* **29**(2), 137–146 (1975)
9. P. Padhi, S.K. Anand, D. Kar, S. Ghosh, S.C. Panigrahi, Modeling structure of Al–Sn Alloy. *Mater. Sci. Forum* **519–521**, 1519–1524 (2006)
10. M.V. Cante, K.S. Cruz, J.E. Spinelli, N. Cheung, A. Garcia, Experimental analysis of the columnar-to-equiaxed transition in directionally solidified Al–Ni and Al–Sn alloys. *Mater. Lett.* **61**(11–12), 2135–2138 (2007)
11. J.E. Spinelli, K.S. Cruz, M.V. Cante, A. Garcia, Primary dendrite arm spacing during transient directional solidification of Al alloys with low redistribution coefficients. *Philos. Mag. Lett.* **89**(12), 779–786 (2009)
12. H.R. Kotadia, J.B. Patel, Z. Fan, E. Doernberg, R. Schmid-Fetzer, Processing of Al–45Sn–10Cu based immiscible alloy by a rheomixing process. *Solid State Phenom.* **141–143**, 529–534 (2008)
13. H.R. Kotadia, E. Doernberg, J.B. Patel, Z. Fan, R. Schmid-Fetzer, Solidification of Al–Sn–Cu based immiscible alloys under intense shearing. *Metall. Mater. Trans. A* **40**(9), 2202–2211 (2009)
14. H.R. Kotadia, J.B. Patel, Z. Fan, E. Doernberg, R. Schmid-Fetzer, Solidification and processing of aluminum based immiscible alloys, in *Aluminum Alloys: Fabrication, Characterization, and Applications*, vol II, ed by W. Yin et al. (The Minerals, Metals & Materials Society, Warrendale, PA 2009), pp. 81–86
15. W. Zhiming, G. Haoran, Z. Guorong, G. Zhongquan, T. Xinying, Temperature-induced anomalous structural changes of Al–12 wt% Sn–4 wt% Si melt and its influence on as-cast structure. *China Foundry* **7**, 138–142 (2010)
16. T. Marrocco, L.C. Driver, S.J. Harris, D.G. McCartney, Microstructure and properties of thermally sprayed Al–Sn-based alloys for plain bearing applications. *J. Therm. Spray Technol.* **15**(4), 634–639 (2006)
17. C. Suryanarayana, T.R. Anantharaman, Solidification of aluminum–germanium alloys at high cooling rates. *J. Mater. Sci.* **5**(11), 992–1004 (1970)
18. F. Hehmann, F. Sommer, B. Predel, Extension of solid solubility in magnesium by rapid solidification. *Mater. Sci. Eng. A* **125**(2), 249–265 (1990)
19. D. Eskin, Q. Du, D. Ruvalcaba, L. Katgerman, Experimental study of structure formation in binary Al–Cu alloys at different cooling rates. *Mater. Sci. Eng. A* **405**, 1–10 (2005)